computed value of S will become larger and consequently the rate constant smaller. One important factor that we did not incorporate into the calculation of S is the changes in the equilibrium configuration of vibrational modes other than the metal-ligand bonds. From the deviations from octahedral symmetry and the ring structures appearing in all the complexes we have mentioned, it is clear that several other ring modes may contribute to S. It is impossible to give a reasonable quantitative estimate for their effect, but undoubtedly S must be larger than the one appearing in our calculation and, therefore, our estimate of the rate constant given here has to be considered as an upper limit.

From this somewhat lengthy discussion of the technical details of the present calculation it is apparent that the numerical values calculated in section IV for the (ls) $\rightleftarrows$ (hs) rate constants should not be taken too seriously as far as absolute numerical magnitude is concerned. It is, however, quite remarkable that the present quantum-mechanical multiphonon theory led to a reasonable order-of-magnitude estimate of the rate constants for this class of processes without the use of any adjustable parameters. In particular, the present theory has been useful in the elucidation of electronic and nuclear contributions to the rate constants for this class of processes. We feel that rate process in condensed phases, such as (ls) $\rightleftarrows$ (hs) crossover considered herein, should be described in terms of multiphonon theories of radiationless transitions, which are more reliable and informative than the conventional absolute reaction rate theory.

References and Notes

(1) Cambi, L.; Cagnoro, A. *Atti Accad. Naz. Lincei* **1931**, *13*, 809.
(2) Martin, R. L.; White, A. H. *Transition Met. Chem.* **1968**, *4*, 113.
(3) Barefield, E. K.; Busch, D. B.; Nelson, S. M. *Q. Rev., Chem. Soc.* **1968**, *22*, 457.
(4) Beattie, J. K.; Sutin, N.; Turner, D. H.; Flynn, G. W. *J. Am. Chem. Soc.* **1973**, *95*, 2052.
(5) Hoselton, M. A.; Drago, R. S.; Wilson, L. J.; Sutin, N. *J. Am. Chem. Soc.* **1976**, *98*, 6967.
(6) Reeder, K. A.; Dose, E. V.; Wilson, L. J. *Inorg. Chem.* **1978**, *17*, 1071.
(7) Dose, E. V.; Hoselton, M. A.; Sutin, N.; Tweedle, M. F.; Wilson, L. J. *J. Am. Chem. Soc.* **1978**, *100*, 1141.
(8) Beattie, J. K.; Binstead, R. A.; West, R. J. *J. Am. Chem. Soc.* **1978**, *100*, 3044.
(9) Dose, E. V.; Murphy, K. M. M.; Wilson, L. J. *Inorg. Chem.* **1976**, *15*, 2622.
(10) Tweedle, M. F.; Wilson, L. J. *J. Am. Chem. Soc.* **1976**, *98*, 4824.
(11) Petty, R. H.; Dose, E. V.; Tweedle, M. F.; Wilson, L. J. *Inorg. Chem.* **1978**, *17*, 1064.
(12) Binstead, R. A.; Beattie, J. K.; Dose, E. V.; Tweedle, M. F.; Wilson, L. J. *J. Am. Chem. Soc.* **1978**, *100*, 5609.
(13) Simmons, M. G.; Wilson, L. J. *Inorg. Chem.* **1977**, *16*, 126.
(14) (a) Austin, K. H.; Beeson, K. W.; Eisenstein, L.; Frauenfelder, H.; Gunsalus, I. C. *Biochemistry* **1975**, *14*, 5355. (b) Jortner, J.; Ulstrup, J. *J. Am. Chem. Soc.* **1979**, *101*, 3744.
(15) Levich, V. G. In "Physical Chemistry: An Advanced Treatise", Eyring, H., Henderson, D., Jost, W., Eds.; Academic Press: New York, 1970; Vol. 9B.
(16) Kestner, N. R.; Logan, J.; Jortner, J. *J. Phys. Chem.* **1974**, *78*, 2148.
(17) Buhks, E.; Bixon, M.; Jortner, J.; Navon, G. *Inorg. Chem.*, **1979**, *18*, 2014.
(18) Griffiths, J. S. "Theory of Transition Metal Ions"; Cambridge University Press: New York, 1961.
(19) Tanabe, Y.; Sugano, S. *J. Phys. Soc. Jpn.* **1954**, *9*, 766.
(20) (a) Jørgensen, C. K. "Absorption Spectra and Chemical Bonding in Complexes"; Pergamon Press: Oxford, 1962. (b) *Prog. Inorg. Chem.* **1962**, *4*, 73.
(21) Gerloch, M.; Slade, R. C. "Ligand Field Parameters"; Cambridge University Press: New York, 1973; p 214.
(22) Dunn, T. M. *Trans. Faraday Soc.* **1961**, *57*, 1441.
(23) Figgis, B. N. "Introduction to Ligand Fields"; Interscience: New York, 1966.
(24) Ferraro, J. R. "Low Frequency Vibrations of Inorganic and Coordination Compounds"; Plenum Press: New York, 1971.
(25) Sinn, E.; Sinn, G.; Dose, E. V.; Tweedle, M. F.; Wilson, L. J. *J. Am. Chem. Soc.* **1978**, *100*, 3375.
(26) Hall, G. R.; Hendrickson, D. N. *Inorg. Chem.* **1976**, *15*, 607.
(27) Leipoldt, J. G.; Coppens, P. *Inorg. Chem.* **1973**, *12*, 2269.
(28) Mealli, C.; Lingafelter, E. C. *Chem. Commun.* **1970**, 885.
(29) Hoselton, M. A.; Wilson, L. J.; Drago, R. S. *J. Am. Chem. Soc.* **1975**, *97*, 1722.
(30) Churchill, M. R.; Gold, K.; Maw, Jr., C. E. *Inorg. Chem.* **1970**, *9*, 1597.

Chiral Discrimination in Excimer Formation

Chieu D. Tran and Janos H. Fendler*

Contribution from the Department of Chemistry, Texas A&M University,
College Station, Texas 77843.

Received November 20, 1978

Abstract: Steady-state and nanosecond time resolved spectroscopy have been used to determine parameters for excimer formation for *N*-[4-(1-pyrene)butanoyl]-D-tryptophan methyl ester (pyr-D-Trp), *N*-[4-(1-pyrene)butanoyl]-L-tryptophan methyl ester (pyr-L-Trp), and their racemate, pyr-DL-Trp, in methanol and for pyr-D-Trp in optically active (*R*)-(−)-2-octanol, (*S*)-(+)-2-octanol, and racemic (*RS*)-(±)-2-octanol. Appreciable differences have been noted between the behavior of the pure enantiomer and its racemate in MeOH. Thus, the rate constant of excimer formation for pyr-DL-Trp, $(6.9 \pm 0.5)\ 10^9\ \mathrm{M}^{-1}\ \mathrm{s}^{-1}$, is greater than those for the pure enantiomers, $(4.0 \pm 0.7)\ 10^9\ \mathrm{M}^{-1}\ \mathrm{s}^{-1}$. The quantum efficiency of pyr-DL-Trp excimer formation ($q_D/q_M = 0.7 \pm 0.1$) is smaller than that for pyr-D-Trp or pyr-L-Trp ($q_D/q_M = 1.1 \pm 0.2$). Differences in equilibrium constants for excimer formation indicated a chiral discrimination energy of 700 cal mol^{-1}. Chiral discrimination originates in differential electrostatic, dispersion, and resonance interactions. Appreciable differences have also been observed in the kinetic and thermodynamic parameters for pyr-D-Trp excimer formation in (*R*)-(−)-2-octanol and (*S*)-(+)-2-octanol.

Introduction

Differences in crystal structures, melting points, boiling points, solubilities, and ^{1}H NMR spectra between a pure enantiomer and its racemate have been recognized for some time.[1-10] Similarly, there are examples of enantiomeric excess dependent reaction rates and product distributions.[6,7] Enantiomeric effects[11] are the results of interactions between two chiral molecules which discriminate between like (*d* with *d* or *l* with *l*) and unlike (*d* with *l* or *l* with *d*) pairs. They have been treated theoretically in terms of short- and long-range nonbonded interactions.[8,10]

Dynamic investigations of photochemical processes[12] can provide a wealth of information on factors which determine enantiomeric discriminations. We have initiated, therefore, systematic studies on excimer formation[13] involving chiral molecules. *N*-[4-(1-Pyrene)butanoyl]-D-tryptophan methyl ester (pyr-D-Trp) and *N*[4-(1-pyrene)butanoyl]-L-tryptophan methyl ester (pyr-L-Trp) have been utilized in the present work. Using steady-state and nanosecond time resolved fluo-

0002-7863/80/1502-2923$01.00/0

rescence spectroscopy leads to the elucidation of rate and equilibrium parameters. Appreciable differences have been observed between the behaviors of the pure enantiomer and its racemate in methanol. Rate and equilibrium parameters for pyr-D-Trp excimer formation have also been determined in optically active (*R*)-(−)-2-octanol, (*S*)-(+)-octanol, and racemic (*RS*)-(±)-2-octanol. Differences in these solvents have been rationalized in terms of hydrogen bonding and diastereomeric equilibrium interactions.[14-22]

Experimental Section

Pyrene-1-butanoyl chloride was prepared by refluxing pyrene-1-butyric acid (2.0 g) and thionyl chloride (4.13 g) in 800 mL of dry benzene for 7 h. The resulting product was recrystallized from dry hexane: yield 1.5 g (71%); mp 73.5–74.5 °C; IR (Nujol) 1800, 840, 665 cm^{-1}.

Pyrene-1-butanoyl chloride (0.603 g), dissolved in benzene (50.0 mL), was added dropwise (30 min) to a dry benzene (100 mL) solution of D-tryptophan methyl ester (1.0 g) and triethylamine (0.398 g), stirred at 5 °C. The reaction mixture was stirred overnight at room temperature and filtered. The filtrate was extracted with benzene, washed twice with 5% aqueous sodium bicarbonate, twice with 2% aqueous acetic acid, and twice with water, and dried over $CaSO_4$ overnight. Subsequent to solvent removal by rotary evaporation, the product, *N*-[4-(1-pyrene)butanoyl]-D-tryptophan methyl ester (pyr-D-Trp), was recrystallized three times from ether–*n*-hexane (1:10 v/v) and dried overnight in vacuo over P_2O_5: yield 0.4 g (42%); mp 156–157 °C; IR (Nujol) 3450, 3350, 1740, 1640, 844 cm^{-1}. pyr-L-Trp was prepared similarly. Anal. Calcd for $C_{32}H_{23}O_3N_2$: C, 78.69; H, 5.74; N, 5.74. Found for pyr-D-Trp: C, 78.66; H, 5.75; N, 5.70. Found for pyr-L-Trp: C, 78.12; H, 5.84; N, 5.62. Specific optical rotation of pyr-D-Trp: $[\alpha]^{25}_{500}$ +12.3°, $[\alpha]^{25}_{400}$ +21.7°. pyr-L-Trp: $[\alpha]^{25}_{500}$ −12.1°, $[\alpha]^{25}_{400}$ −23.3° (*c* 0.499, MeOH). *N*-[4-(1-Pyrene)butanoyl]glycine methyl ester (pyr-Gly) was prepared analogously. Its purity was established by IR, absorption, and fluorescence spectroscopy. (*S*)-(+)-2-Octanol and (*R*)-(−)-2-octanol were obtained from Aldrich and used without further purification: $[\alpha]_D^{25}$ +(7.8 ± 0.1) and (−7.8 ± 0.1)° for (*S*)-(+)-2-octanol and (*R*)-(−)-2-octanol, respectively. (*RS*)-(±)-2-Octanol (Sigma) was washed with concentrated sulfuric acid, saturated aqueous solution of potassium bicarbonate, and copious amounts of distilled water. Following these washings it was vacuum distilled twice. No optical activity within experimental error was observed for (*RS*)-(±)-2-octanol. All other reagents were the best available spectroanalyzed grade and used as received.

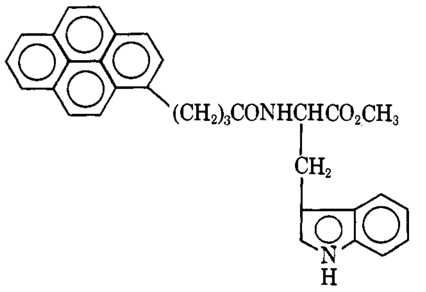

pyr-D-Trp or pyr-L-Trp

Absorption spectra were taken on a Cary 118C spectrophotometer. ORD spectra were determined on a Jasco J-20 spectropolarimeter. Steady-state fluorescence excitation and emission spectra were obtained on a SPEX Fluorolog spectrofluorimeter using the E/R mode. Generally 2.5-mm slits and 3-nm bandwidth were used.

Fluorescence lifetimes were determined by means of a modified ORTEC 9200 single photon counting nanosecond time resolved fluorescence spectrometer with the output displayed on a multichannel analyzer. Excitation wavelengths were selected by the use of appropriate filters (Ditric Optics, Inc.) having 5-nm half-height bandwidth. Fluorescence lifetimes were calculated on an on-line digital PDP-11/10 computer using the method-of-moments program. The temperature was maintained to ±0.1 °C by water circulation. Fluorescence excitation and emission spectra, nanosecond time resolved spectra, as well as lifetimes were determined on degassed samples. Degassing was carried out on a high-vacuum line using repeated freeze-pump-thaw cycles.

Data Treatments and Results

Increasing the concentrations of pyr-D-Trp, pyr-L-Trp, pyr-DL-Trp, or pyr-Gly in methanol resulted in the appearance of blue, structureless emission bands centered at 470 nm (Figure 1). Similar spectral behavior was observed for pyr-D-Trp in optically active or racemic 2-octanol. The longer wavelength bands originate in pyrene–pyrene-type excited dimers or excimers, D*, formed in the association of ground, M, and excited state, M*, monomers.[12,13] Formation of indole–pyrene exciplexes can be excluded since the behavior of pyr-Gly (no indole) is qualitatively similar to that of pyr-Trp. Equation 1 describes the reaction scheme as given by Birks.[23]

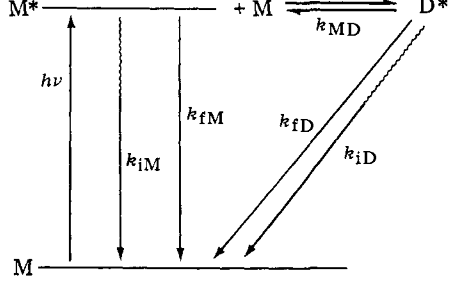

(1)

Rate parameters k_{fM}, k_{iM}, and k_{DM} govern the fluorescence of M*, the internal quenching of M*, and excimer formation. Similarly, k_{fD}, k_{iD}, and k_{MD} represent rate constants for the fluorescence of D*, the internal quenching of D*, and the regeneration of M*. For convenience direct decays of M* and D* to M are given by the equations

$$k_M = k_{fM} + k_{iM} \tag{2}$$

$$k_D = k_{fD} + k_{iD} \tag{3}$$

The quantum intensities of monomer fluorescence per initial excited molecules of M at time *t* is given by the equation

$$I_M(t) = \frac{k_{fM}\{\lambda_2 - (k_M + k_{DM}[M])\}}{\lambda_2 - \lambda_1} e^{-\lambda_1 t} + \frac{k_{fM}\{\lambda_2 - (k_M + k_{DM}[M])\}}{\lambda_2 - \lambda_1} Ae^{-\lambda_2 t} \tag{4}$$

$$A = \frac{k_M + k_{DM}[M] - \lambda_1}{\lambda_2 - (k_M + k_{DM}[M])}$$

Similarly, the quantum intensity of excimer fluorescence per initial excited molecules of M at time *t* is given by the equation

$$I_D(t) = \frac{k_{fD}k_{DM}[M]}{\lambda_2 - \lambda_1}(e^{-\lambda_1 t} - e^{-\lambda_2 t}) \tag{5}$$

The rate parameter, λ_1, was experimentally obtained by the deconvolution of fluorescence decay due either to the monomer (at 390 nm) or the excimer (at 470 nm) of pyr-D-Trp, pyr-L-Trp, pyr-DL-Trp, and pyr-Gly. Although the rate parameter λ_2 can be evaluated from the buildup of excimer fluorescence, it is more convenient to approximate it from the equation

$$t_{max} = \ln(\lambda_2/\lambda_1)/(\lambda_2 - \lambda_1) \tag{6}$$

where t_{max} is the time delay between the maximum of the exciting light pulse and the fluorescence emission maximum of the excimer. Using the known value of λ_1, and t_{max}, λ_2 was evaluated by successive approximation using a computer program. Decay parameters λ_1 and λ_2 were shown[23] to relate to rate parameters by the equations

$$\lambda_1 + \lambda_2 = k_M + k_D + k_{MD} + k_{DM}[M] \tag{7}$$

$$\lambda_1\lambda_2 = k_Dk_{DM}[M] + k_Mk_{MD} + k_Mk_D \tag{8}$$

Figure 2 shows plots of the data for pyr-L-Trp and pyr-DL-Trp

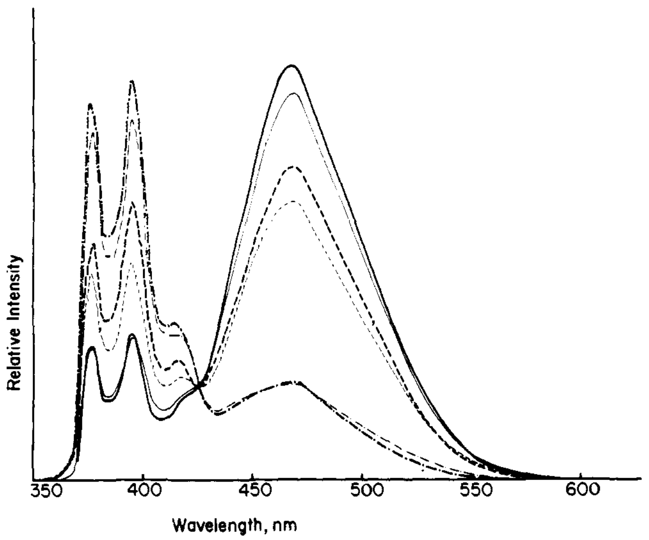

Figure 1. Fluorescence emission of 1.0 × 10^{-3} M pyr-L-Trp (-----), 1.0 × 10^{-3} M pyr-DL-Trp (-·-·-), 5.0 × 10^{-3} M pyr-L-Trp (- - -), 5.0 × 10^{-3} M pyr-DL-Trp (- - -), 1.0 × 10^{-2} M pyr-L-Trp (—), and 1.0 × 10^{-2} M pyr-DL-Trp (—) in MeOH, excited at 342 nm, normalized at 425 nm. pyr-DL-Trp solutions were obtained by mixing equal volumes of equal concentrations of pyrD-Trp and pyr-L-Trp.

according to eq 7 and 8. Values for pyr-D-Trp and pyr-Gly were plotted similarly. These plots allow calculations of k_{DM} and k_D for each system. Additional parameters for excimer formation may be evaluated from steady-state measurements of relative quantum yields. Relative quantum yields of the excimer, Φ_D, and monomer, Φ_M, were obtained by comparing the area under the monomer with that under the excimer, normalizing the spectra at 425 nm and taking area$_D$ + area$_M$ = 1.0.[24-26] The insert in Figure 3 shows plots of excimer (Φ_D) to monomer (Φ_M) quantum yield ratios as functions of pyr-D-Trp, pyr-L-Trp, and pyr-DL-trp concentrations. K_1 values were calculated from the slopes of these plots:

$$\Phi_D/\Phi_M = K_1[M] \qquad (9)$$

Equilibrium constants K_1, K, and K_e are defined and related to each other by the equations

$$K_e = k_{DM}/(k_{MD} + k_D) = [D^*]/([M][M^*]) \qquad (10)$$

$$K = (k_D/k_M)K_e \qquad (11)$$

$$K_1 = K(q_D/q_M) \qquad (12)$$

where q_D and q_M are the quantum efficiencies of the excimer and monomer fluorescence, respectively. These latter values were evaluated from the equation

$$1/\Phi_D = 1/q_D + (C_h/q_D)(1/[M]) \qquad (13)$$

where C_h is the "half-value" concentration at which $I_M = \frac{1}{2}q_M$ and $I_D = \frac{1}{2}q_D$. Figure 3 shows treatment of the data according to eq 13. Table I collects the determined parameters for excimer formation for pyr-D-Trp, pyr-L-Trp, pyr-DL-Trp, and pyr-Gly in methanol at 25 °C. Similar parameters for pyr-D-Trp excimer formation in optically active (R)-(−)-2-octanol, (S)-(+)-2-octanol, and racemic (RS)-(±)-2-octanol at 16.5, 27.0, 39.0, 45.0, and 52.0 °C are given in Tables II-VI. Ratios of dimer to monomer yields increase as functions of pyr-D-Trp concentrations differently in (R)-(−)-2-octanol, (S)-(+)-2-octanol, and racemic (RS)-(±)-2-octanol. The data at 16.5, 39.0, and 52.0 °C, plotted according to eq 9, are shown in Figure 4.

Equations 14 and 15 relate k_{DM} and k_{MD} to the activation energies of excimer formation, W_{DM}, and decomposition, W_{MD}, respectively.

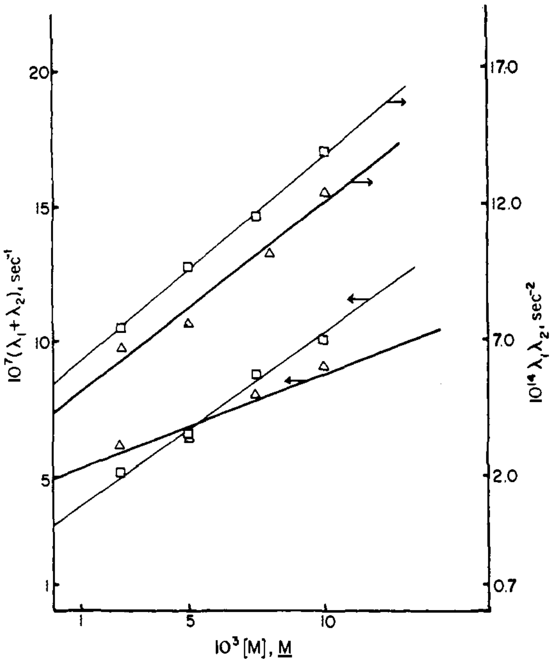

Figure 2. Plots of the data for pyr-L-Trp (△) and pyr-DL-Trp (□) according to eq 7 and 8.

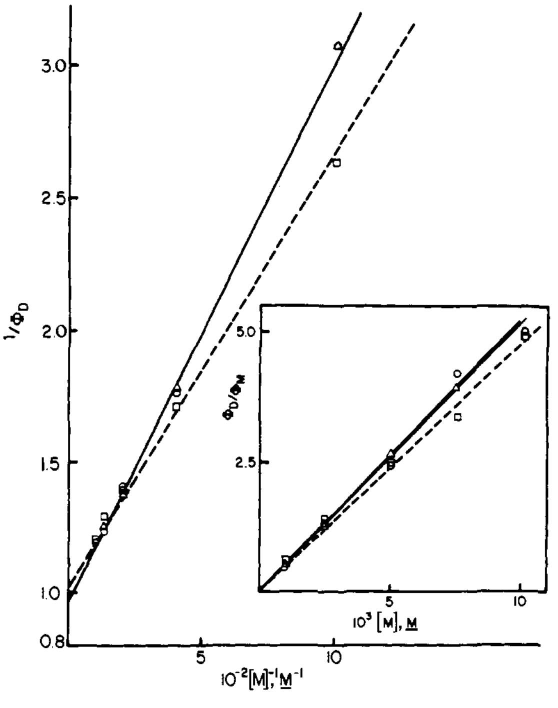

Figure 3. Treatment of the data for pyr-D-Trp (△), pyr-L-Trp (○), and pyr-DL-Trp (□) according to eq 13 and 9 (insert).

$$k_{DM} = k'_{DM}\exp(-W_{DM}/kT) \qquad (14)$$

$$k_{MD} = k'_{MD}\exp(-W_{MD}/kT) \qquad (15)$$

where k is Boltzmann's constant, $k'_{DM}/k'_{MD} = \exp(\Delta S/R)$. Differences between the activation energies of excimer decomposition and formation give the excimer binding energy, B:

$$W_{MD} - W_{DM} = B = -\Delta H/N \qquad (16)$$

where ΔH is the thermodynamic energy difference between M* + M and D* (i.e., it is the enthalpy of activation for excimer formation) and N is Avogadro's number. Equations 17 and 18 interrelate and allow the calculation of the various

Table I. Rate and Equilibrium Constants for Excimer Formation in MeOH at 25.0 °C[a]

	pyr-D-Trp	pyr-L-Trp	pyr-DL-Trp[b]	pyr-Gly
k_{DM}, M^{-1} s^{-1}	$(4.0 \pm 1.0)10^9$	$(4.0 \pm 0.7)10^9$	$(6.9 \pm 0.5)10^9$	$(7.0 \pm 0.6)10^9$
k_{MD}, s^{-1}	$(3.3 \pm 0.4)10^7$	$(2.6 \pm 0.4)10^7$	$(1.6 \pm 0.2)10^7$	$(7.8 \pm 1.0)10^6$
K, M^{-1}	$(4.8 \pm 0.6)10^2$	$(4.8 \pm 0.6)10^2$	$(6.7 \pm 0.9)10^2$	$(5.3 \pm 0.7)10^2$
q_D/q_M	1.1 ± 0.2	1.1 ± 0.2	0.7 ± 0.1	1.1 ± 0.2
k_M, s^{-1}	$(3.2 \pm 0.4)10^6$	$(3.6 \pm 0.5)10^6$	$(4.5 \pm 0.6)10^6$	$(3.9 \pm 0.5)10^6$
k_D, s^{-1}	$(2.1 \pm 0.3)10^7$	$(2.0 \pm 0.3)10^7$	$(1.2 \pm 0.1)10^7$	$(1.8 \pm 0.3)10^7$
K_e, M^{-1}	$(0.7 \pm 0.1)10^2$	$(0.9 \pm 0.1)10^2$	$(2.5 \pm 0.3)10^2$	$(2.8 \pm 0.4)10^2$
K_1, M^{-1}	$(5.2 \pm 0.7)10^2$	$(5.2 \pm 0.7)10^2$	$(4.7 \pm 0.6)10^2$	$(5.7 \pm 0.8)10^2$
C_h, M	$(2.1 \pm 0.3)10^{-3}$	$(2.1 \pm 0.3)10^{-3}$	$(1.5 \pm 0.2)10^{-3}$	$(1.9 \pm 0.3)10^{-3}$

[a] See eq 1-3 and 9-13 for definitions. [b] Obtained by mixing equal volumes and equal concentrations of pyr-D-Trp and pyr-L-Trp.

Table II. Rate and Equilibrium Constants for pyr-D-Trp Excimer Formation in (*S*)-(+)-2-Octanol, (*R*)-(−)-2-Octanol, and (*RS*)-(±)-2-Octanol at 16.5 °C

	in (*S*)-(+)-2-octanol	in (*R*)-(−)-2-octanol	in (*RS*)-(±)-2-octanol
k_{DM}, M^{-1} s^{-1}	$(5.2 \pm 0.4)10^8$	$(8.1 \pm 0.5)10^8$	$(7.0 \pm 0.4)10^8$
k_{MD}, s^{-1}	$(2.7 \pm 0.4)10^6$	$(3.0 \pm 0.2)10^6$	$(4.8 \pm 0.3)10^6$
k_M, s^{-1}	$(5.3 \pm 0.5)10^6$	$(5.3 \pm 0.5)10^6$	$(5.2 \pm 0.3)10^6$
k_D, s^{-1}	$(9.9 \pm 0.4)10^6$	$(1.01 \pm 0.07)10^7$	$(1.43 \pm 0.05)10^7$
K, M^{-1}	78 ± 5	$(1.16 \pm 0.3)10^2$	$(2.03 \pm 0.3)10^2$
K_1, M^{-1}	45 ± 4	$(52 \pm 5)10^2$	50 ± 4
K_e, M^{-1}	$(1.96 \pm 0.05)10^2$	$(1.70 \pm 0.06)10^2$	$(1.43 \pm 0.04)10^2$
q_D/q_M	0.58 ± 0.02	0.45 ± 0.03	0.25 ± 0.02
C_h, M	(1.28 ± 0.05)-10^{-2}	(8.57 ± 0.05)-10^{-3}	$(0.49 \pm 0.04)10^{-2}$

Table III. Rate and Equilibrium Constants for pyr-D-Trp Excimer Formation in (*S*)-(+)-2-Octanol, (*R*)-(−)-2-Octanol, and (*RS*)-(±)-2-Octanol at 27.0 °C

	in (*S*)-(+)-2-octanol	in (*R*)-(−)-2-octanol	in (*RS*)-(±)-2-octanol
k_{DM}, M^{-1} s^{-1}	$(7.3 \pm 0.5)10^8$	$(9.9 \pm 0.5)10^8$	$(8.0 \pm 0.2)10^8$
k_{MD}, s^{-1}	$(4.9 \pm 0.3)10^6$	$(5.8 \pm 0.5)10^6$	$(5.8 \pm 0.7)10^6$
k_M, s^{-1}	$(5.5 \pm 0.7)10^6$	$(5.5 \pm 0.7)10^6$	$(1.0 \pm 0.8)10^7$
k_D, s^{-1}	$(9.8 \pm 0.9)10^6$	$(1.1 \pm 0.9)10^7$	$(1.9 \pm 0.8)10^7$
K, M^{-1}	$(1.4 \pm 0.6)10^2$	$(1.14 \pm 0.7)10^2$	$(2.5 \pm 0.8)10^2$
K_1, M^{-1}	54 ± 1.0	64.6 ± 3.0	62 ± 2.0
K_e, M^{-1}	$(1.48 \pm 0.05)10^2$	$(1.71 \pm 0.05)10^2$	$(1.38 \pm 0.05)10^2$
q_D/q_M	0.38 ± 0.02	0.57 ± 0.03	0.25 ± 0.02
C_h, M	$(8.76 \pm 0.6)10^{-3}$	$(7.04 \pm 0.5)10^{-3}$	$(6.73 \pm 0.7)10^{-3}$

activation parameters:

$$\frac{k_{DM}}{k_{MD}} = K_e = \frac{k'_{DM}}{k'_{MD}} \exp\left(\frac{W_{MD} - W_{DM}}{kT}\right) \tag{17}$$

$$\Delta G = -kT \ln K_e = \Delta H - T\Delta S \tag{18}$$

These values are given in Table VII.

Discussion

Taking advantage of intermolecular excimer formation, two kinds of chiral recognitions have been investigated in the present work. In the first kind, differences in kinetic and thermodynamic parameters have been determined for excimer formation between enantiomerically pure and racemic pyr-Trp in methanol. This type of differentiation between a pure enantiomer and its racemate is referred to as the enantiomeric effect.[6,7] In the second kind of experiments, analogous photophysical parameters have been obtained for pyr-Trp excimer formation in optically active and racemic 2-octanols. Differences in (*R*)-(−)-2-octanol, (*S*)-(+)-2-octanol, and (*RS*)-(±)-2-octanol are the consequence of solvent-induced diastereomeric interactions.

Table IV. Rate and Equilibrium Constants for pyr-D-Trp Excimer Formation in (*S*)-(+)-2-Octanol, (*R*)-(−)-2-Octanol, and (*RS*)-(±)-2-Octanol at 39.0 °C

	in (*S*)-(+)-2-octanol	in (*R*)-(−)-2-octanol	in (*RS*-(±)-2-octanol
k_{DM}, M^{-1} s^{-1}	$(1.4 \pm 0.2)10^9$	$(1.6 \pm 0.2)10^9$	$(1.5 \pm 0.3)10^9$
k_{MD}, s^{-1}	$(9.6 \pm 0.5)10^6$	$(1.10 \pm 0.5)10^7$	$(9.7 \pm 0.4)10^6$
k_M, s^{-1}	$(6.3 \pm 0.5)10^6$	$(6.2 \pm 0.4)10^6$	$(6.2 \pm 0.5)10^6$
k_D, s^{-1}	$(1.3 \pm 0.4)10^7$	$(1.2 \pm 0.3)10^7$	$(1.5 \pm 0.5)10^7$
K, M^{-1}	$(1.1 \pm 0.2)10^2$	$(0.8 \pm 0.1)10^2$	$(1.5 \pm 0.3)10^2$
K_1, M^{-1}	84 ± 5	94 ± 5	84 ± 5
K_e, M^{-1}	$(1.4 \pm 0.5)10^2$	$(1.5 \pm 0.5)10^2$	$(1.6 \pm 0.5)10^2$
q_D/q_M	0.74 ± 0.02	0.70 ± 0.02	0.56 ± 0.03
C_h, M	(8.74 ± 0.05)-10^{-3}	(7.50 ± 0.03)-10^{-3}	$(0.67 \pm 0.05)10^{-3}$

Table V. Rate and Equilibrium Constants for pyr-D-Trp Excimer Formation in (*S*)-(+)-2-Octanol, (*R*)-(−)-2-Octanol, and (*RS*)-(±)-2-Octanol at 45.0 °C

	in (*S*)-(+)-2-octanol	in (*R*)-(−)-2-octanol	in (*RS*)-(±)-2-octanol
k_{DM}, M^{-1} s^{-1}	$(1.5 \pm 0.4)10^9$	$(1.7 \pm 0.3)10^9$	$(1.6 \pm 0.4)10^9$
k_{MD}, s^{-1}	$(1.3 \pm 0.5)10^7$	$(1.2 \pm 0.3)10^7$	$(1.2 \pm 0.1)10^7$
k_M, s^{-1}	$(6.6 \pm 0.5)10^6$	$(6.2 \pm 0.4)10^7$	$(6.7 \pm 0.4)10^7$
k_D, s^{-1}	$(1.4 \pm 0.3)10^7$	$(1.4 \pm 0.1)10^7$	$(1.6 \pm 0.4)10^7$
K, M^{-1}	$(1.1 \pm 0.1)10^2$	$(1.69 \pm 0.1)10^2$	$(1.4 \pm 0.1)10^2$
K_1, M^{-1}	96 ± 3	107 ± 4	74 ± 4
K_e, M^{-1}	$(1.2 \pm 0.2)10^2$	$(1.4 \pm 0.3)10^2$	$(1.3 \pm 0.1)10^2$
q_D/Q_M	0.88 ± 0.02	0.64 ± 0.01	0.24 ± 0.05
C_h, M	(9.17 ± 0.05)-10^{-3}	$5.93 \pm 0.01)10^{-3}$	$(3.3 \pm 0.01)10^{-3}$

Table VI. Rate and Equilibrium Constants for pyr-D-Trp Excimer Formation in (*S*)-(+)-2-Octanol, (*R*)-(−)-2-Octanol, and (*RS*)-(±)-2-Octanol at 52.0 °C

	in (*S*)-(+)-2-octanol	in (*R*)-(−)-2-octanol	in (*RS*)-(±)-2-octanol
k_{DM}, M^{-1} s^{-1}	$(1.6 \pm 0.1)10^9$	$(1.9 \pm 0.2)10^9$	$(1.7 \pm 0.2)10^9$
k_{MD}, s^{-1}	$(1.0 \pm 0.1)10^7$	$(7.9 \pm 0.4)10^6$	$(7.9 \pm 0.2)10^6$
k_M, s^{-1}	$(6.8 \pm 0.4)10^6$	$(6.7 \pm 0.5)10^6$	$(6.8 \pm 0.4)10$
k_D, s^{-1}	$(1.5 \pm 0.5)10^7$	$(1.4 \pm 0.3)10^7$	$(1.7 \pm 0.5)10^7$
K, M^{-1}	$(1.5 \pm 0.1)10^2$	$(2.2 \pm 0.5)10^2$	$(1.3 \pm 0.4)10^2$
K_1, M^{-1}	$(1.1 \pm 0.4)10^2$	$(1.3 \pm 0.2)10^2$	$(1.2 \pm 0.1)10^2$
K_e, M^{-1}	$(1.6 \pm 0.3)10^2$	$(2.4 \pm 0.3)10^2$	$(0.9 \pm 0.1)10^2$
q_D/q_M	0.7 ± 0.2	0.6 ± 0.1	0.9 ± 0.2
C_h, M	$(6.8 \pm 0.1)10^3$	$(4.6 \pm 0.5)10^3$	$(7.9 \pm 0.4)10^3$

The most significant accomplishment of the present work is the demonstration of the extreme sensitivity of excimer formation in quantifying stereoselectivities. Pyrene-type excimers, investigated in the present study, are formed by collisional interactions of electronically excited singlet and ground-state pyr-Trp monomers and assume parallel sandwich-type configurations.[12,13] Excimer formation efficiency is strongly dependent upon the optimization of configurational and conformational interactions between ground- and excited-state monomers. Since excimer formation is a diffusion-controlled process, differences in $k_{\rm DM}$ values (eq 1) between pyr-D-Trp (or pyr-L-Trp) and pyr-DL-Trp in methanol or that between (*R*)-(−)-2-octanol, (*S*)-(+)-2-octanol, and (*RS*)-(±)-2-octanol for pyr-D-Trp are due to differences in the reaction probability per encounter, p, or that in viscosities, η:[27,28]

$$k_{\rm DM} = 8RTp/3000\eta \qquad (19)$$

Once formed, the excimers are diastereomeric with respect to each other (pyr*-D-Trp, pyr-D-Trp; pyr*-L-Trp; pyr-L-Trp; pyr*=D-Trp, pyr-L-Trp; pyr-D-Trp, pyr*-L-Trp). Similarly, pyr-D-Trp is diastereomeric with respect to the solvent (pyr*-D-Trp, (*R*)-(−)-2-octanol; pyr*-D-Trp, (*S*)-(+)-2-octanol; pyr*-D-Trp, (*RS*)-(±)-2-octanol). Diastereomeric differences have not been discernible by any other measurements for the systems investigated in the present study. A similar situation has recently been encountered in the intermolecular energy transfer from terbium(III) to europium(III) complexes of enantiomerically pure and racemic aspartic acids.[29] Above pH 5.5, energy transfer was more efficient to the racemic aspartic acid complex than to their enantiomerically pure counterparts, even though no ground-state differences could be detected.[30]

Free energies of excimer formation have been calculated from eq 18 to be −2.6 and −3.3 kcal mol^{-1} for pyr-D-Trp (or pyr-L-Trp) and for pyr-DL-Trp, respectively. The difference, 700 cal mol^{-1}, corresponds to the chiral discrimination energy. This value is within the range of that causing noticeable differences in reaction rates.[6] The observed enantiomeric discrimination in excimer formation is a composite effect originating in electrostatic, dispersion, and resonance interactions. Resonance interaction is likely to contribute to the chiral discrimination since excited and unexcited molecules can be coupled by the emission and absorption of a photon.[8] Resonance discrimination may arise from the differential coupling of like (pyr-D-Trp with pyr-D-Trp or pyr-L-Trp with pyr-L-Trp) and unlike (pyr-D-Trp with pyr-L-Trp or pyr-L-Trp with pyr-D-Trp) pairs. The magnitude of resonance discrimination has been estimated to be rather small and the effect has not previously been experimentally verified.

Interactions of chiral pyr-D-Trp with chiral 2-octanols are given by the equations

$$\text{pyr-D-Trp} + (R)\text{-}(-)\text{-2-octanol} \overset{K_{\rm R}}{\rightleftharpoons} \text{pyr-D-Trp}\cdot(R)\text{-}(-)\text{-2-octanol} \qquad (20)$$

$$\text{pyr-D-Trp} + (S)\text{-}(+)\text{-2-octanol} \overset{K_{\rm S}}{\rightleftharpoons} \text{pyr-D-Trp}\cdot(S)\text{-}(+)\text{-2-octanol} \qquad (21)$$

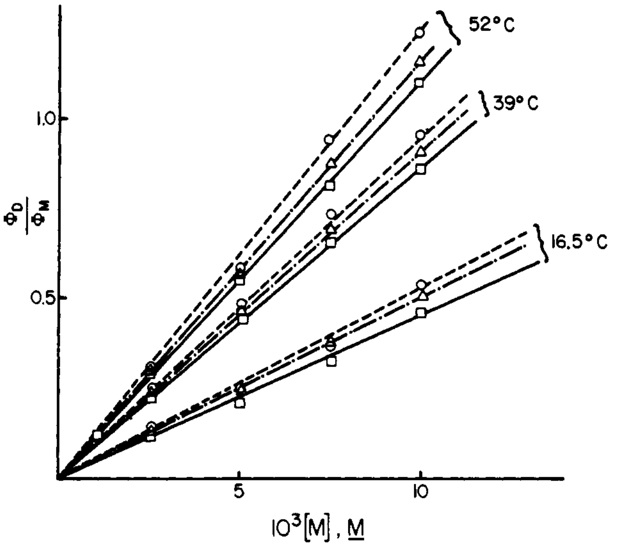

Figure 4. Treatment of the data for pyr-D-Trp in (*S*)-(+)-2-octanol (□), (*R*)-(−)-2-octanol (○), and (*RS*)-(±)-2-octanol (△) according to eq 9.

Table VII. Thermodynamic Parameters for pyr-D-Trp Excimer Formation in (*S*)-(+)-2-Octanol, (*R*)-(−)-2-Octanol, and (*RS*)-(±)-2-Octanol

	in (*S*)-(+)-2-octanol	in (*R*)-(−)-2-octanol	in (*RS*)-(±)-2-octanol
$W_{\rm DM}$, eV	0.20 ± 0.01	0.27 ± 0.01	0.22 ± 0.02
$W_{\rm MD}$, eV	0.34 ± 0.03	0.44 ± 0.02	0.38 ± 0.02
B, eV	0.14 ± 0.03	0.16 ± 0.04	0.15 ± 0.02
Δ*H*, kcal/mol	−3.2 ± 0.2	−3.8 ± 0.3	−3.5 ± 0.2
Δ*S*, eu	−3.0 ± 0.3	−0.33 ± 0.1	−2.0 ± 0.3
Δ*G*,[a] kcal/mol	−2.9 ± 0.3	−3.1 ± 0.2	−2.9 ± 0.2

[a] Calculated at 27.0 °C.

Selective solvation, contact interaction, complex formation, and hydrogen bonding may contribute to differences between $K_{\rm R}$ and $K_{\rm S}$. Differential hydrogen bonding can be visualized as shown. Hydrogen-bonding interactions, causing solvent-induced configurational activities, have been studied and shown to result in approximately 300 cal/mol discrimination energy.[31] The observed difference in the enthalpy of activation for the pyr-D-Trp excimer formation in (*R*)-(−)-2-octanol and (*S*)-(+)-2-octanol, 600 cal/mol (Table VII), is greater than that observed for discrimination energies involving hydrogen-bonding interaction. An additional or alternative source of discrimination may originate in differential complexation between pyr-D-Trp and the enantiomeric alcohols. Indeed, formation of weak complexes between pyrene and alcohols has been reported.[32] Steric differences between the diastereomeric

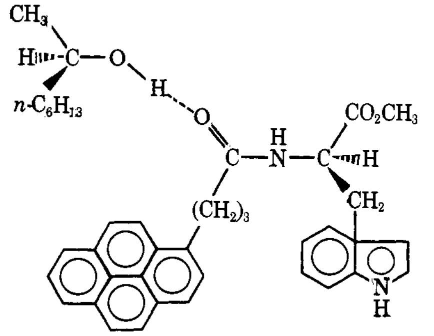

(*R*)-(−)-2-octanol and pyr-D-Trp

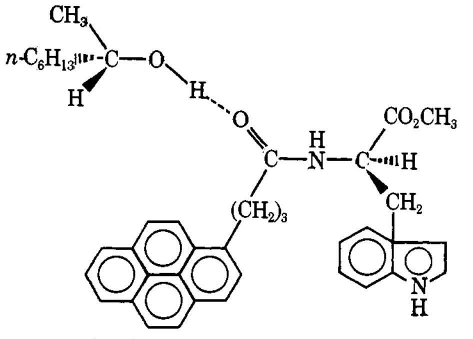

(*S*)-(+)-2-octanol and pyr-D-Trp

structures are manifest in different kinetic and thermodynamic parameters for pyr-D-Trp excimer formation in (R)-(−)-2-octanol and (S)-(+)-2-octanol.

Acknowledgment is made to the donors of the Petroleum Research Fund, administered by the American Chemical Society, for support of this research by a New Directions in Fundamental Research grant.

References and Notes

(1) Horeau, A. *Tetrahedron Lett.* **1969**, 3121.

(2) William, T.; Pitcher, R. G.; Bommer, P.; Gutzwiller, J.; Uskokovic, M. *J. Am. Chem. Soc.* **1969**, *91*, 1871.

(3) Collet, A.; Brienne, M.-J.; Jacques, J. *Bull. Soc. Chim. Fr.* **1972**, 127.

(4) Horeau, A.; Gvette, J. P. *Tetrahedron* **1974**, *30*, 1923.

(5) Kabachnik, M. I.; Mastryvkora, T. A.; Fedin, E. I.; Vaisberg, M. S.; Movozov, L. L.; Petrovsky, P. V.; Shipor, A. E. *Tetrahedron* **1976**, *32*, 1719.

(6) Wynberg, H.; Feringa, B. *Tetrahedron* **1976**, *32*, 2831.

(7) Wynberg, H. *Chimia* **1976**, *30*, 445.

(8) Craig, D. P.; Mellor, D. P. *Fortschr. Chem. Forsch.* **1976**, *63*, 1.

(9) Mason, S. F. *Annu. Rep. Prog. Chem., Sect. A* **1978**, *73*, 53.

(10) Kuroda, R.; Mason, S. F.; Rodger, C. D.; Seal, R. H. *Chem. Phys. Lett.* **1978**, *57*, 1.

(11) Terms chirodiastaltic diastereotropic have been alternatively used to describe the part of interaction between two chiral molecules which discriminate between like and unlike pairs.[8]

(12) (a) Birks, J. B. "Photophysics of Aromatic Molecules"; Interscience: New York, 1973. (b) Birks, J. B., Ed. "Organic Molecular Photophysics"; Interscience: New York, 1973.

(13) Birks, J. B. *Rep. Prog. Phys.* **1975**, *38*, 903.

(14) Craig, D. P.; Power, E. A.; Thrunamachandran, T. *Chem. Phys. Lett.* **1974**, *27*, 149.

(15) Bosnich, B. *J. Am. Chem. Soc.* **1967**, *89*, 6143.

(16) Hayward, L. D.; Totty, R. N. *Can. J. Chem.* **1971**, *49*, 623.

(17) Claesson, S.; Hayward, L. D. *Chem. Phys. Lett.* **1973**, *20*, 85.

(18) Schipper, P. E. *Inorg. Chim. Acta* **1975**, *14*, 161.

(19) Schipper, P. E. *Chem. Phys. Lett.* **1975**, *30*, 323.

(20) Hayward, L. D.; Claesson, S. *Chem. Scr.* **1976**, *9*, 21.

(21) Mason, S. F. *Chem. Phys. Lett.* **1975**, *32*, 201.

(22) Schipper, P. E. *Mol. Phys.* **1975**, *29*, 1705.

(23) Birks, J. B.; Dyson, D. J.; Munro, I. H. *Proc. R. Soc. London, Ser. A* **1963**, *275*, 575.

(24) Birks, J. B.; Christophorou, L. G. *Spectrochim. Acta* **1963**, *19*, 401.

(25) Birks, J. B.; Christophorou, L. G. *Proc. R. Soc. London, Ser. A* **1963**, *274*, 552.

(26) Aladekomo, J. B.; Birks, J. B. *Proc. R. Soc. London, Ser. A* **1964**, *284*, 551.

(27) Noyes, R. M. *Prog. React. Kinet.* **1961**, *1*, 138.

(28) Alwatter, A. M.; Lumb, M. D.; Birks, J. B. In ref 12b, p 403.

(29) Brittain, H. G. *Inorg. Chem.* **1979**, *18*, 1740.

(30) We have also determined parameters for tryptophan to pyrene intramolecular energy transfer in pyr-D-Trp, pyr-L-Trp, and pyr-DL-Trp. Energy-transfer efficiencies of 44.4 ± 0.2 and 45.7 ± 0.2% were obtained for pyr-D-Trp (or pyr-L-Trp) and for pyr-DL-Trp, respectively. Rate constants for the energy transfer, $(1.43 \pm 0.05)10^9$ s^{-1} for pyr-D-Trp (or pyr-L-Trp) and $(2.39 \pm 0.06)10^9$ s^{-1} for pyr-DL-Trp, also showed enantiomeric discriminations. These effects are related to differences in the environments of pyr-Trp. In an optically pure solution of pyr-D-Trp, all the molecules are surrounded by their own kinds. There is a similar situation for pyr-L-Trp. Conversely, in a racemic solution some pyr-D-Trp is surrounded by pyr-L-Trp and some pyr-L-Trp encounters pyr-D-Trp. Since these experiments were carried out at 1.0×10^{-5} M solute concentration, the observed discriminations could not be readily rationalized. Following the referees' comments and the advice of the Editor we have decided to postpone the publication of these and related data until we develop a satisfactory model to rationalize them.

(31) Dwyer, F. P.; Gyarfas, E. C.; O'Dwyer, M. F. *Nature (London)* **1951**, *167*, 1036. Davies, N. R.; Dwyer, F. P. *Trans. Faraday Soc.* **1953**, *49*, 180. Barnes, G. T.; Backhouse, J. R.; Dwyer, F. P.; Gyarfas, E. C. *J. Proc. R. Soc. N.S.W.* **1955**, *89*, 151.

(32) Lianos, P.; Georghiou, S. *Photochem. Photobiol.* **1979**, *29*, 843.

Unified View of Marcus Electron Transfer and Mulliken Charge Transfer Theories in Organometallic Chemistry. Steric Effects in Alkylmetals as Quantitative Probes for Outer-Sphere and Inner-Sphere Mechanisms

S. Fukuzumi, C. L. Wong, and J. K. Kochi*

Contribution from the Department of Chemistry, Indiana University, Bloomington, Indiana 47405. *Received July 11, 1979*

Abstract: Electron transfer rate constants for various homoleptic organometals, especially tetraalkyltin, tetraalkyllead, and dialkylmercury, with tris(1,10-phenanthroline)iron(III), hexachloroiridate(IV), and tetracyanoethylene are compared under standard reaction conditions. Although electron transfer from alkylmetals to FeL_3^{3+} (where L = 1,10-phenanthroline) follows the Marcus correlation with the predicted slope $\alpha = 0.5$ for an outer-sphere mechanism, both $IrCl_6^{2-}$ and TCNE show deviations which vary with the steric hindrance in the alkylmetal, RM. Inner-sphere mechanisms for the latter are also indicated by electron-transfer rates which can be 10^{7-9} times faster than those predicted by the Marcus equation using measured values of the reduction potentials and the reorganizational energies of $IrCl_6^{2-}$ and TCNE. This conclusion is supported by differences in the cleavage selectivities S(Et/Me) for a series of methylethyltin compounds as well as the activation parameters for electron transfer. The Mulliken theory of charge transfer (CT) in TCNE complexes is used to evaluate steric effects in various alkylmetals. The difference ΔE in the charge transfer transition energy $h\nu_{CT}$ of the CT complex relative to that of a reference alkylmetal is assigned to steric effects on the interaction energy associated with ion-pair formation in the successor complex for the inner-sphere mechanism. The result is the linear free energy relationship, $\Delta G^{\ddagger} = \Delta G^{\circ} + \Delta E$, which can be applied to the kinetics of electron transfer from alkylmetals in the absence of steric effects. The unification of Marcus electron transfer and Mulliken charge transfer theories in this manner allows outer-sphere and inner-sphere mechanisms of electron transfer to evolve from a single viewpoint.

Introduction

Historically, the theories of electron transfer in chemical reactions have been developed largely from two quite separate and independent approaches. On one hand, the evolution from inorganic chemistry of oxidation–reduction mechanisms pertaining to transition-metal complexes has led to the Marcus theory, as well as the intervalence transfer theory of Hush.[1,2] The other approach, tracing back to the charge-transfer theory of Mulliken, stems from organic substrates and deals mainly with electronic transitions.[3] Mulliken's theory employs the intermolecular distance between donor and acceptor as the only

0002-7863/80/1502-2928$01.00/0